

RAPID COMMUNICATION | OCTOBER 17 2023

Crystallization of FAPbI_3 : Polytypes and stacking faults

Special Collection: [2023 JCP Emerging Investigators Special Collection](#)

Paramvir Ahlawat  



J. Chem. Phys. 159, 151102 (2023)

<https://doi.org/10.1063/5.0165285>

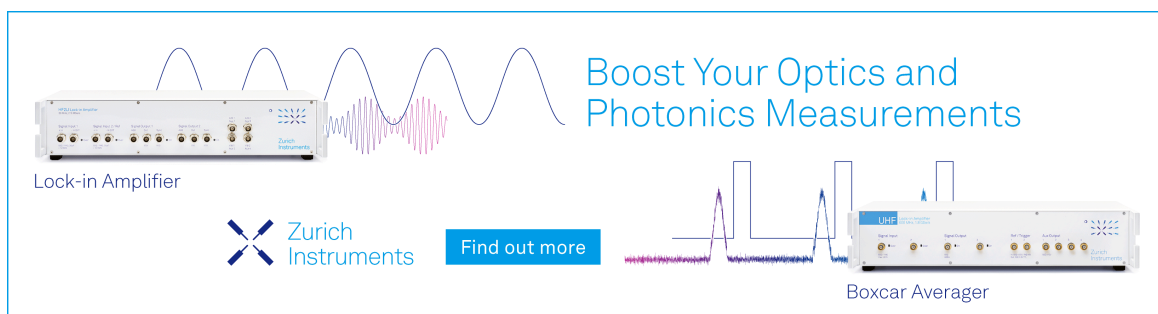


View
Online




Export
Citation

CrossMark



Boost Your Optics and
Photonics Measurements

Lock-in Amplifier

 Zurich
Instruments

[Find out more](#)

Boxcar Averager

Crystallization of FAPbI₃: Polytypes and stacking faults

Cite as: J. Chem. Phys. 159, 151102 (2023); doi: 10.1063/5.0165285

Submitted: 27 June 2023 • Accepted: 15 September 2023 •

Published Online: 17 October 2023



View Online



Export Citation



CrossMark

Paramvir Ahlawat^{a)}

AFFILIATIONS

SNSF Post-doc Mobility Fellow, Yusuf Hamied Department of Chemistry, University of Cambridge, Cambridge CB2 1EW, United Kingdom and Institute of Chemical Sciences and Engineering, Ecole Polytechnique Federale de Lausanne (EPFL), CH-1015 Lausanne, Switzerland

Note: This paper is part of the 2023 JCP Emerging Investigators Special Collection.

^{a)} Author to whom correspondence should be addressed: paramvir.chem@gmail.com

ABSTRACT

Molecular dynamics simulations are performed to study the crystallization of formamidinium lead iodide. From all-atom simulations of the crystal growth process and the δ - α -phase transitions, we try to reveal the formation of various stack-faulted intermediate defected structures and report various polytypes of formamidinium lead iodide that are observed from simulations.

© 2023 Author(s). All article content, except where otherwise noted, is licensed under a Creative Commons Attribution (CC BY) license (<http://creativecommons.org/licenses/by/4.0/>). <https://doi.org/10.1063/5.0165285>

I. INTRODUCTION

Formamidinium lead iodide (FAPbI₃)^{1,2} based perovskite solar cells (PSC)^{3–8} have emerged as the most promising cheaper photovoltaic technology with certified solar to power conversion efficiencies for single-junction 26.1%^{8–13} and perovskite-silicon tandem solar cells reaching ~34%.^{8,14–16} This material has two commonly known phases: black phase and hexagonal yellow phase. Among these, thermodynamically stable hexagonal-FAPbI₃ is a photo-inactive material and consists of face-sharing Pb–I octahedral chains surrounded by FA⁺ cations. Alternatively, the metastable black-FAPbI₃ is made of corner-sharing Pb–I octahedra and a champion photo-active material commonly used to make highly efficient and stable PSCs. The phase transition temperature from the yellow to black phase is ~150 °C. Over the past decade, one of the main quests in perovskite photovoltaics has been to synthesize and stabilize phase-pure or alloyed black-FAPbI₃. A broad range of processing methodologies and additives have been explored to make a defects-free black-FAPbI₃ and simultaneously avoid the formation of hexagonal structures. Regardless of the abundance of experiments, perovskite electronics suffer from the problem of limited stability and reproducibility. It is apparent from regular research papers of PSCs where control samples are shown to degrade within hours during the solar cell operations. This is mainly due to the lack of understanding and control over their synthesis process where one

of the critical challenges is to eliminate the formation of hexagonal face-sharing structures and their alternative polytypes.^{17–25} Therefore, it is necessary to study their formation process which can help to make reproducible and stable FAPbI₃ based PSCs. The temporal and spatial resolution required to study the dynamical process of crystallization: limit the usage of current state-of-the-art experimental techniques and a huge challenge to design and perform experiments for these materials.^{26,27} An alternate approach of molecular dynamics (MD) simulations^{23,28–36} can help better understand the atomic level details of complex crystallization process. In this work, we perform brute-force MD simulations and try to understand the formation of intermediate polytypic structures of FAPbI₃ which play an essential role in the efficiency and long-term stability of PSCs. Experimental synthesis of black-FAPbI₃ involves various steps, and conducting all-atom MD simulations of an entire experimental process is a challenging task. This study is limited to two cases: (a) crystal growth and (b) hexagonal (δ) to the cubic (α)-phase transition of FAPbI₃.

II. CRYSTAL GROWTH

We start with the growth process of FAPbI₃ and carry out seeded simulations.^{31,34} During the usual manufacturing processes,³⁸ solvents are expelled quickly to form thin films of perovskites. This is commonly achieved either using typical coating

techniques (for example, spin-coating), anti-solvents, and high-temperature annealing. Removal of solvent molecules creates conditions of very high supersaturation and leads to the onset of multiple nucleation and growth events. We could only simulate parts of this complicated growth process in this work. To set-up our simulations, we prepare crystalline seeds of cubic and hexagonal-FAPbI₃ and interface them with a homogeneous mixture of Pb²⁺, I⁻ and FA⁺ ions, shown in Fig. 1(a). All atom MD simulations are performed with an AMOEBA^{39–46} polarizable inter-atomic potential of FAPbI₃, details are provided in the supplementary information. From simulations, we observe a net growth of crystalline phase over both {111}-facet of cubic phase and {001}-facet of hexagonal phase, illustrated in Figs. 1(a)–1(d). We analyse these simulations with the time evolution of different types of Pb–I octahedra;⁴⁷ see Fig. 1(e). This representation allows

to quantify the formation of hexagonal and cubic-FAPbI₃ structures with face-sharing and corner-sharing, respectively, where edge-sharing are fingerprints of various precursor intermediate phases⁴⁸ observed in experiments. We find that both face-sharing and corner-sharing octahedra increase with the decrease of edge-sharing ones. This is a direct observation of the formation of mixed 4H and 9R-like polytypes, see Fig. 1(d) and supplementary movie M1. Similar intra-grain structures are also observed in electron microscopic and X-ray experiments.^{24,49–52} However, experiments have not established the crystallization mechanism of these structures. Therefore, a key insight comes out from simulations is that the mixed face-corner-sharing Pb–I structures possibly form during crystal growth in perovskites on either {111}-face of cubic-phase or unconverted hexagonal-phase of FAPbI₃. To further characterize the growth process, free energies surfaces (FES) are

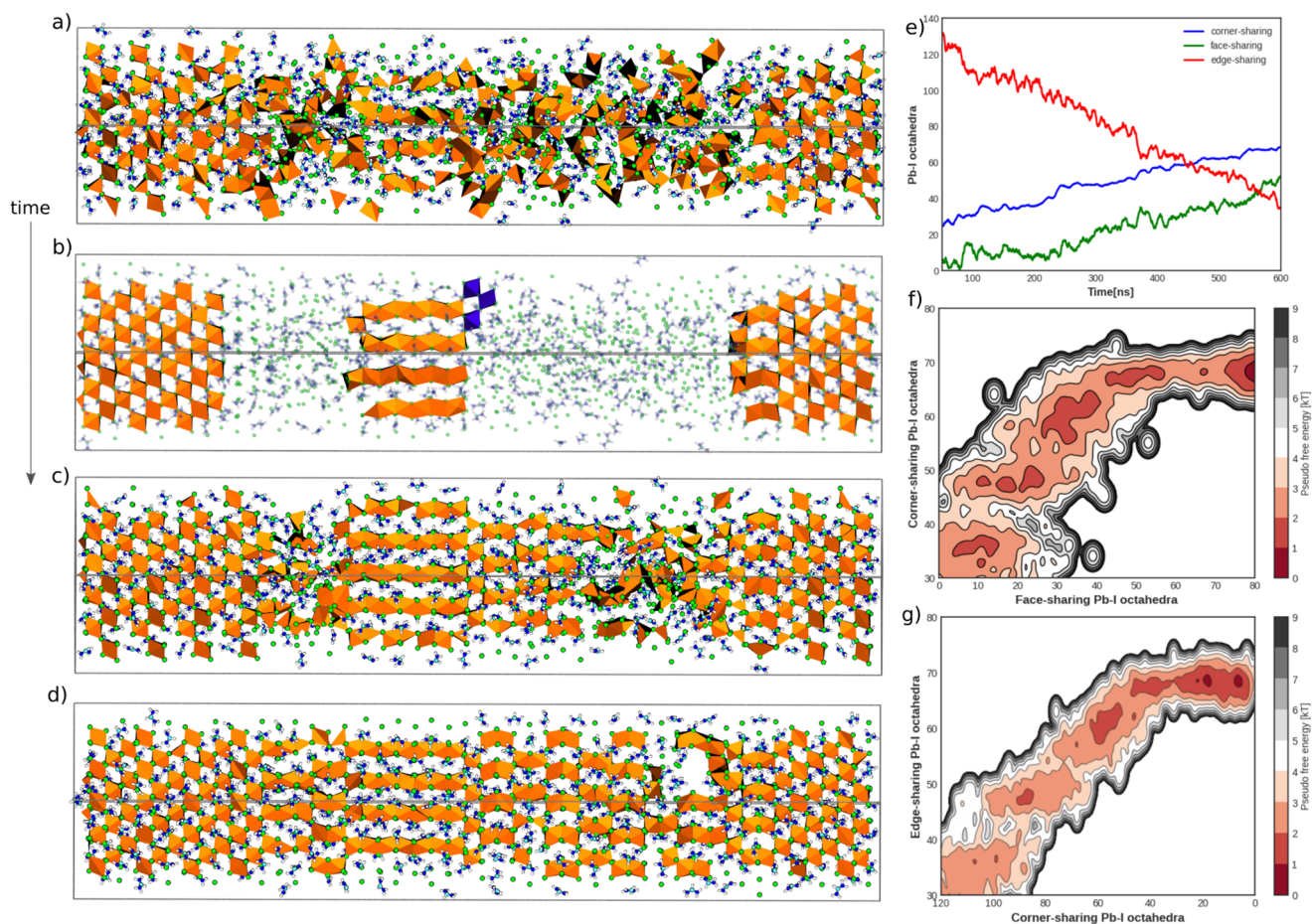


FIG. 1. Crystal Growth: Figures (a)–(d) display the atomistic picture of the time evolution of a typical growth process, where (a) is the initial configuration of the homogeneous mixtures of precursor ions in between seeds of hexagonal (face-sharing in middle) and cubic-FAPbI₃ (on corners). Figure (b) highlights the initial nucleation on face-sharing seed. Figure (c) shows the growth of polytype and figure (d) depicts the complete formation of polytypes. All figures are generated with the VMD software.³⁷ Pb–I configurations are depicted as orange octahedra with green iodine at corners. Violet color Pb–I octahedra in figure (b) are shown to guide the eye. FA⁺ cations are shown with balls and sticks configuration. Figure (e) shows the time evolution of edge-sharing, corner-sharing and face-sharing Pb–I octahedra during crystallization process. Figure (f) and (g) are the pseudo free energy profiles.

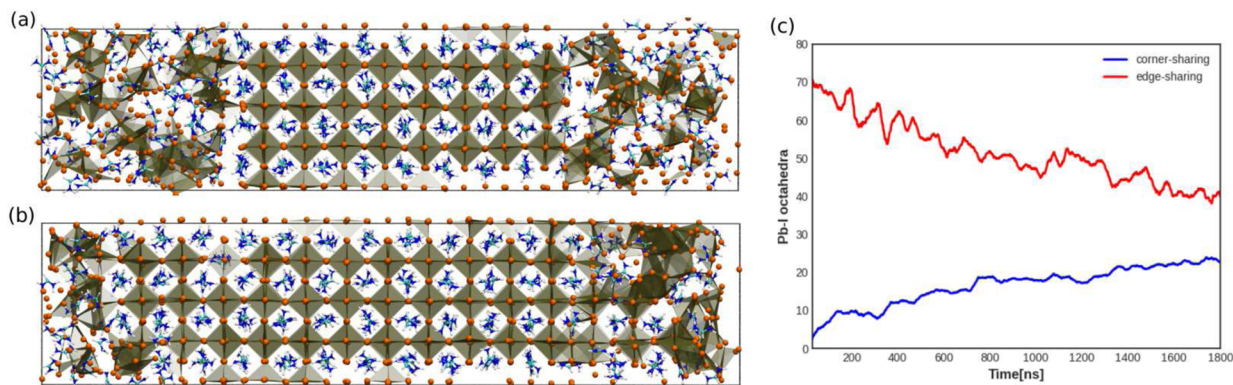


FIG. 2. Crystal Growth: Figures (a) and (b) shows the crystallization of corner-sharing Pb–I octahedra on {100}- α -FAPbI₃, where (a) is the initial configuration of the homogeneous mixtures of precursor ions interfaced with cubic-FAPbI₃. Figure (b) shows the newly grown perovskite. Figure (c) shows the time evolution of edge-sharing and corner-sharing Pb–I octahedra during the growth process. Figures (a) and (b) are created with the VMD software.³⁷ Pb–I configurations are depicted as brown color octahedra with orange iodine spheres at corners. FA⁺ cations are shown with balls and sticks configuration.

constructed with equation^{53–55} $F = -k_B T \log p(O_{\text{type of Pb-I octahedra}})$, where $p(O_{\text{type of Pb-I octahedra}})$ is the probability distribution of the face-sharing, edge-sharing and corner-sharing octahedra. From these 2D pseudo-FES in Figs. 1(f) and 1(g), it can be noticed that the polytype layers are separated by free energy barriers. Now, upon careful observations of the simulated trajectories, we recognize that the polytype growth starts from the nucleation of corner-sharing structure on seed of hexagonal-phase and face-sharing structures on seed of cubic-phase. To further characterize this phenomena, we calculate the free energy profile for the growth of a single layer of polytype, see supplementary Fig. 1(c). As can be noticed from supplementary Fig. 1(c), that the growth of one layer is separated by a free energy barrier from its starting configuration. Therefore, indicating that once a two-dimensional type nucleation starts to form complete Pb–I octahedra on surface of respective seeds [see Fig. 1(b)], in-plane polytype layer forms with a continuous growth, see supplementary Fig. 1(c). This feature is also broadly present in the free energy surface in Fig. 1, where multiple free energy minima are associated with the polytype layers, see Figs. 1(f) and 1(g). Furthermore, we also realize that defects can form during this growth process which may act as degradation centers during the operation of PSCs. A defected interface structure can be directly seen in Fig. 1(d) with the unconverted Pb–I octahedra. Therefore, the crystallized structures from this study can be further used to understand defects^{56,57} and their effects on degradation of FAPbI₃. Apart from {111}-facet of cubic-phase, we carry out simulations of seeded growth on {100}-facet, however we did not observe formation of any hexagonal-face-sharing structures, see Fig. 2.

III. δ TO α -PHASE TRANSITION OF FAPbI₃

In the course of synthesis process, thermodynamically stable δ -phase is frequently crystallized first and later converted to perovskite.^{9,12} It is essential to comprehend the atomic-level details of this process. Previously, Professor JB Goodenough and co-workers^{19,59,60} have experimentally demonstrated that face-sharing perovskite structures can transform into various polytypes and

eventually convert to fully corner-sharing structures during high-pressure synthesis. On the basis of these experimental observations, we carry out MD simulations of direct phase transitions from face-sharing to corner-sharing phases of FAPbI₃. However, solid-solid nucleation/phase-transitions are often characterized as rare events, meaning required simulation times may go beyond the capabilities of the current computational architecture. To overcome this problem, we take inspiration from earlier computer simulations of polytypes^{20,61} and explore the potential energy surface by altering potential energy surface.^{62–67} All simulation details are provided in the supplementary information. We start with an initial configuration where a few corner-sharing structures are inserted in a sizeable face-sharing structure of FAPbI₃; see supplementary Fig. 2(a). Brute-force MD simulations are performed at accelerated temperatures.^{54,68–71} With increasing temperatures, face-sharing octahedra transform into corner-sharing ones either by sliding of Pb–I layers or melted-like intermediates, see supplementary Fig. 2. This gives rise to the formation of various hexagonal 4H, 6H, 8H, 10H, 12H, and 9R-like perovskite polytypes,^{24,72–76} their mixtures and stacking faults,⁵⁰ see atomic dynamics in supplementary movies M2 and M3. We identify their structures based on ratio of cubic(c) to hexagonal(h) stacking for example 4H(chch),¹⁹ and 6H(cchch),²⁴ see supplementary Fig. 3. Here, Figs. 3(a)–3(i) shows the identified crystalline structures for the supercell of 1296 atoms. Similar structures are also detected from simulations of larger supercells up to 5000 atoms. In addition, we carry out finite-temperature *ab initio* MD simulations of these structures with the density functional theory,^{77–79} and find that the observed structures are also stable in their original configurations at finite-temperature DFT potential energy surface. Therefore predicted polymorphs have a high probability of formation during the crystallization of FAPbI₃. Most notable 4H, 6H, 8H polytypes and stack-faulted intra-grain defects seen here in simulations: are already verified with experiments.^{24,76,80} This substantiates our simulations and encourages experimentalists to synthesize the predicted higher-order polytypes towards a complete understanding of the phase diagram of FAPbI₃.

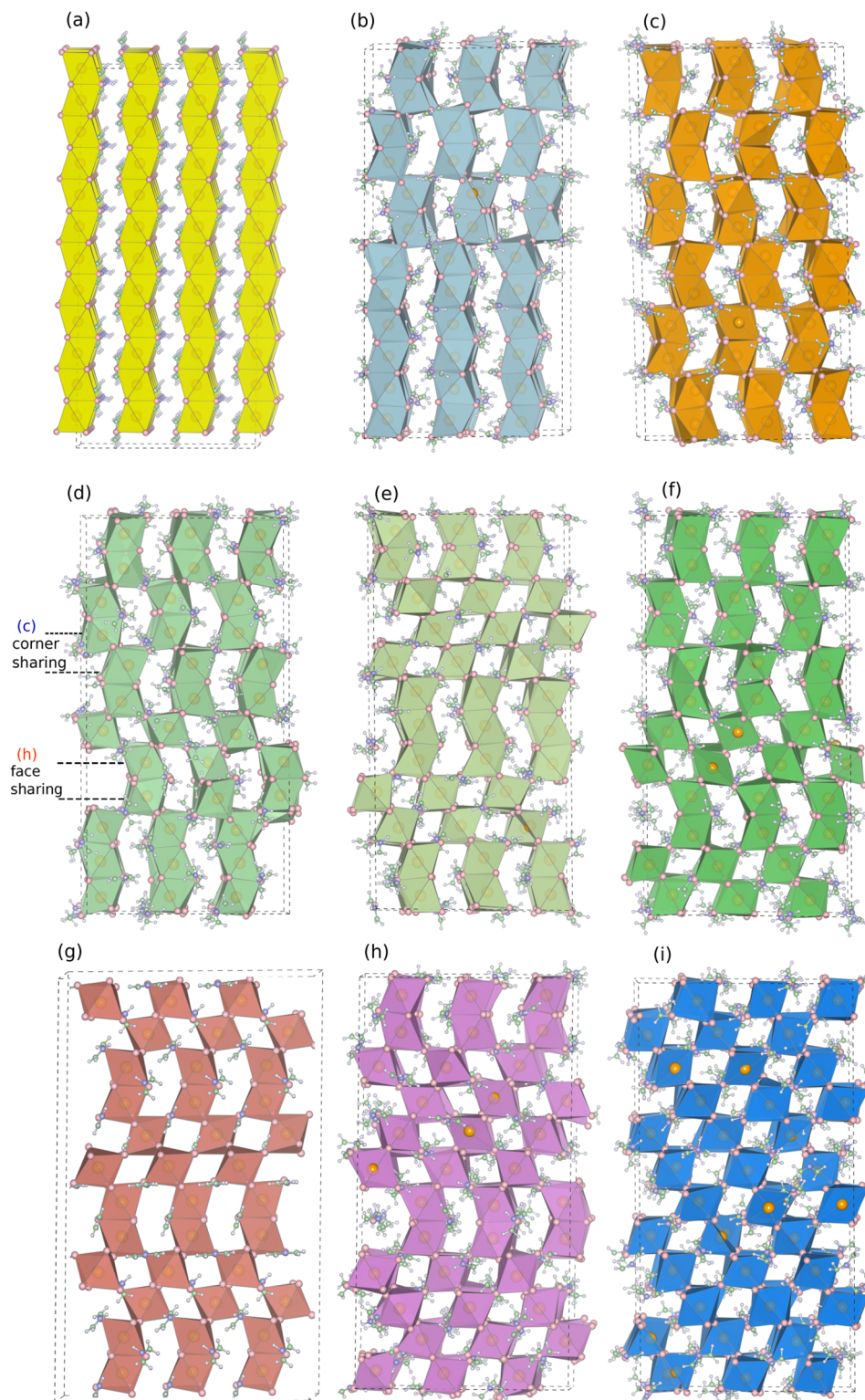


FIG. 3. δ to α -phase transition: Figures (a)–(i) show the predicted structures of various polytypes during the phase transitions of a supercell of 1296 atoms. All figures are made with the structures from AIMD simulations using VESTA software.⁵⁸ Pb–I configurations are depicted as octahedra with iodine at corners. FA⁺ cations are shown with balls and sticks configuration.

IV. DISCUSSIONS

We have taken elementary steps in understanding the crystallization of FAPbI₃. First, our simulations reveal that the 4H and 9R-like polytypes could form on {111}-facet of black FAPbI₃. Whereas, {100}-facet is found to be primarily dominated by the growth of the perovskite corner-sharing octahedra. It could be one of the crucial insights that emerged from simulations. To simplify this observation: it is well established that the efficiency and stability of FAPbI₃-based electronic devices directly depend on the amount of corner-sharing octahedra. Therefore, to extract the maximum solar power from a stable FAPbI₃, one might have to design synthesis recipes that limit the formation of {111}-orientation and maximize the {100}-FAPbI₃. We note that our current work has been limited for guiding the experiments, however simulation methodology presented here can be comfortably extended to study the effect of various additives and therefore help in designing better experimental recipes. Secondly, we simulate the phase transition from δ to α -phase of FAPbI₃ and found that various polytypes/stack-faulted structures can crystallise going from hexagonal (2H) to cubic(3R/3C)-FAPbI₃. These phases are found to have complicated stacking sequences of mixed corners and face-sharing octahedra. We report the crystal structures of the higher-order polytypes and the mixed long-ranged stack-faulted structures. The reported structures can help to provide a better understanding of the complete phase diagram of FAPbI₃. At first, it is essential to obtain the phase diagram of FAPbI₃ with respect to temperature, because high-temperature annealing is an important step for the production of PSCs. Secondly, to make reproducible PSCs, it is critical to comprehend the impact of frequently employed additives (for example cesium,⁸¹ chloride,⁸² bromide,⁸³ and methylenediammonium^{84,85}) on the stabilization of various polytypes of FAPbI₃. Furthermore, despite a plethora of experiments, it is not yet established why PSCs manufactured by the direct conversion of δ to α phase yield inferior efficiencies and poor stability compared to the ones produced by using additives in the crystallization process. Our simulations identified that the defects are associated with the crystallization of polytypes, either from the growth process or direct solid-solid (δ - α) phase transitions. In the end, we note that previously Professor Daan Frenkel and co-workers⁸⁶ calculated that the stabilization of stack-faulted structures could also depend on the size of thin-films, and it may also require longer times to anneal out these structures in FAPbI₃ thin-films. Moreover, polytypism is widely present in nature^{87,88} and industrial materials⁸⁹ with applications ranging from transistors⁹⁰ to quantum computing⁹¹ to spin-glasses⁷⁵ to superconductivity.⁹²⁻⁹⁴ Especially, previous fundamental research on polytypism in silicon-carbide⁹⁵ and oxide perovskites⁹⁶ have demonstrated the stabilization of meta-stable cubic phases: one of the central topics for PSCs. Therefore, to produce highly stable industrial-scale FAPbI₃ based PSCs, a great deal of future fundamental research is needed and an in-depth understanding of the effects of commonly used additives^{10,12,13} on the crystallization of these structures.

SUPPLEMENTARY MATERIAL

See the supplementary material for details about the methodology to perform force field based MD simulations and *ab initio* MD

simulations, atomistic movies extracted from MD simulations, and input files are provided for running MD simulations.

ACKNOWLEDGMENTS

I am greatly thankful to Dr. Zhi Wang for his enormous help with Tinker-GPU code. I am sincerely thankful to insightful discussions, guidance and encouragement from Professor Michael Graetzel, Professor Chris Pickard, Professor Henry Snaith, Professor David Mitzi, Professor Bing-Wei Mao, Dr. M. Ibrahim Dar, Professor Joanne Etheridge, Professor Anthony Stone, Professor Kui Zhao, and Professor RJ Cava. I thank Dr. Pascal Schouwink, Dr. Hong Zhang, Dr. Huyen Pham, Dr. Zi-Ang Nan, Dr. Liang Chen and Dr. Joel Smith for discussions on the formation of polytypes in halide perovskites. I am greatly thankful to Professors David Wales, Angelos Michaelides, and Department of Theoretical Chemistry at University of Cambridge for providing necessary computational resources through Rogue-GPU cluster. This research is funded and supported by Swiss National Science Foundation through post-doc mobility Fellowship No. P500PN_206693.

AUTHOR DECLARATIONS

Conflict of Interest

The author has no conflicts to disclose.

Author Contributions

Paramvir Ahlawat: Conceptualization (lead); Data curation (lead); Formal analysis (lead); Funding acquisition (lead); Investigation (lead); Methodology (lead); Validation (lead); Visualization (lead); Writing – original draft (lead).

DATA AVAILABILITY

Everything reported in this work is reproducible. All kinds of input files, structures, atomic trajectories, simulation materials to reproduce any parts of this study are available on open access server Zenodo:10.5281/zenodo.8211663, 10.5281/zenodo.8330696, 10.5281/zenodo.8330700, 10.5281/zenodo.8330704, 10.5281/zenodo.8330706, 10.5281/zenodo.8330708 and also from the author.

REFERENCES

- 1 S. Wang, D. B. Mitzi, C. A. Feild, and A. Guloy, "Synthesis and characterization of [NH₂C(I):NH₂]₃MI₅ (M = Sn, Pb): Stereochemical activity in divalent tin and lead halides containing single (110) perovskite sheets," *J. Am. Chem. Soc.* **117**, 5297–5302 (1995).
- 2 C. C. Stoumpos, C. D. Malliakas, and M. G. Kanatzidis, "Semiconducting tin and lead iodide perovskites with organic cations: Phase transitions, high mobilities, and near-infrared photoluminescent properties," *Inorg. Chem.* **52**, 9019–9038 (2013).
- 3 A. Kojima, K. Teshima, Y. Shirai, and T. Miyasaka, "Organometal halide perovskites as visible-light sensitizers for photovoltaic cells," *J. Am. Chem. Soc.* **131**, 6050–6051 (2009).
- 4 J.-H. Im, C.-R. Lee, J.-W. Lee, S.-W. Park, and N.-G. Park, "6.5% efficient perovskite quantum-dot-sensitized solar cell," *Nanoscale* **3**, 4088 (2011).

- ⁵J.-W. Lee, D.-J. Seol, A.-N. Cho, and N.-G. Park, "High-efficiency perovskite solar cells based on the black polymorph of $\text{HC}(\text{NH}_2)_2\text{PbI}_3$," *Adv. Mater.* **26**, 4991–4998 (2014).
- ⁶T. M. Koh, K. Fu, Y. Fang, S. Chen, T. C. Sum, N. Mathews, S. G. Mhaisalkar, P. P. Boix, and T. Baikie, "Formamidinium-containing metal-halide: An alternative material for near-IR absorption perovskite solar cells," *J. Phys. Chem. C* **118**, 16458–16462 (2014).
- ⁷N. Pellet, P. Gao, G. Gregori, T.-Y. Yang, M. K. Nazeeruddin, J. Maier, and M. Grätzel, "Mixed-organic-cation perovskite photovoltaics for enhanced solar-light harvesting," *Angew. Chem.* **126**, 3215–3221 (2014).
- ⁸Best Research-Cell Efficiency Chart | Photovoltaic Research | NREL.
- ⁹H. Lu, Y. Liu, P. Ahlawat, A. Mishra, W. R. Tress, F. T. Eickemeyer, Y. Yang, F. Fu, Z. Wang, C. E. Avalos, B. I. Carlsen, A. Agarwalla, X. Zhang, X. Li, Y. Zhan, S. M. Zakeeruddin, L. Emsley, U. Rothlisberger, L. Zheng, A. Hagfeldt, and M. Grätzel, "Vapor-assisted deposition of highly efficient, stable black-phase FAPbI_3 perovskite solar cells," *Science* **370**, eabb8985 (2020).
- ¹⁰J. Jeong, M. Kim, J. Seo, H. Lu, P. Ahlawat, A. Mishra, Y. Yang, M. A. Hope, F. T. Eickemeyer, M. Kim, Y. J. Yoon, I. W. Choi, B. P. Darwich, S. J. Choi, Y. Jo, J. H. Lee, B. Walker, S. M. Zakeeruddin, L. Emsley, U. Rothlisberger, A. Hagfeldt, D. S. Kim, M. Grätzel, and J. Y. Kim, "Pseudo-halide anion engineering for α - FAPbI_3 perovskite solar cells," *Nature* **592**, 381–385 (2021).
- ¹¹J. J. Yoo, G. Seo, M. R. Chua, T. G. Park, Y. Lu, F. Rotermund, Y.-K. Kim, C. S. Moon, N. J. Jeon, J.-P. Correa-Baena, V. Bulović, S. S. Shin, M. G. Bawendi, and J. Seo, "Efficient perovskite solar cells via improved carrier management," *Nature* **590**, 587–593 (2021).
- ¹²J. Park, J. Kim, H.-S. Yun, M. J. Paik, E. Noh, H. J. Mun, M. G. Kim, T. J. Shin, and S. I. Seok, "Controlled growth of perovskite layers with volatile alkylammonium chlorides," *Nature* **616**, 724–730 (2023).
- ¹³Y. Zhao, F. Ma, Z. Qu, S. Yu, T. Shen, H.-X. Deng, X. Chu, X. Peng, Y. Yuan, X. Zhang, and J. You, "Inactive $(\text{PbI}_2)_2$ RbCl stabilizes perovskite films for efficient solar cells," *Science* **377**, 531–534 (2022).
- ¹⁴F. Sahli, J. Werner, B. A. Kamino, M. Bräuninger, R. Monnard, B. Paviet-Salomon, L. Barraud, L. Ding, J. J. Diaz Leon, D. Sacchetto, G. Cattaneo, M. Despeisse, M. Boccard, S. Nicolay, Q. Jeangros, B. Niesen, and C. Ballif, "Fully textured monolithic perovskite/silicon tandem solar cells with 25.2% power conversion efficiency," *Nat. Mater.* **17**, 820–826 (2018).
- ¹⁵A. Al-Ashouri, E. Köhnen, B. Li, A. Magomedov, H. Hempel, P. Caprioglio, J. A. Márquez, A. B. Morales Vilches, E. Kasparavicius, J. A. Smith, N. Phung, D. Menzel, M. Grischek, L. Kegelmann, D. Skroblin, C. Gollwitzer, T. Malin-auskas, M. Jošt, G. Matič, B. Rech, R. Schlattmann, M. Topič, L. Korte, A. Abate, B. Stannowski, D. Neher, M. Stollerfoht, T. Unold, V. Getautis, and S. Albrecht, "Monolithic perovskite/silicon tandem solar cell with >29% efficiency by enhanced hole extraction," *Science* **370**, 1300–1309 (2020).
- ¹⁶S. Albrecht, M. Saliba, J. P. Correa Baena, F. Lang, L. Kegelmann, M. Mews, L. Steier, A. Abate, J. Rappich, L. Korte, R. Schlattmann, M. K. Nazeeruddin, A. Hagfeldt, M. Grätzel, and B. Rech, "Monolithic perovskite/silicon-heterojunction tandem solar cells processed at low temperature," *Energy Environ. Sci.* **9**, 81–88 (2016).
- ¹⁷H. Baumhauer, "XII. Über die verschiedenen Modifikationen des Carborundums und die Erscheinung der Polytypie," *Z. Kristallogr. - Cryst. Mater.* **55**, 249–259 (1915).
- ¹⁸P. Krishna and A. R. Verma, "Crystal-polymorphism in one dimension," *Phys. Status Solidi B* **17**, 437–477 (1966).
- ¹⁹J. Goodenough, J. Kafalas, and J. Longo, "High-pressure synthesis," in *Preparative Methods in Solid State Chemistry* (Elsevier, 1972), pp. 1–69.
- ²⁰C. N. R. Rao, "Some interesting phase transitions in solids," *Bull. Mater. Sci.* **3**, 75–90 (1981).
- ²¹T. Negas and R. Roth, "Phase equilibria and structural relations in the system BaMnO_{3-x} ," *J. Solid State Chem.* **3**, 323–339 (1971).
- ²²J. Darriet, M. Drillon, G. Villeneuve, and P. Hagenmuller, "Interactions magnétiques dans des groupements binucléaires du Ruthénium +V," *J. Solid State Chem.* **19**, 213–220 (1976).
- ²³S. Ramasesha and C. N. R. Rao, "Monte Carlo simulation of polytypes," *Philos. Mag.* **36**, 827–833 (1977).
- ²⁴P. Gratia, I. Zimmermann, P. Schouwink, J.-H. Yum, J.-N. Audinot, K. Sivula, T. Wirtz, and M. K. Nazeeruddin, "The many faces of mixed ion perovskites: Unraveling and understanding the crystallization process," *ACS Energy Lett.* **2**, 2686–2693 (2017).
- ²⁵L. Merten, A. Hinderhofer, T. Baumeler, N. Arora, J. Hagenlocher, S. M. Zakeeruddin, M. I. Dar, M. Grätzel, and F. Schreiber, "Quantifying stabilized phase purity in formamidinium-based multiple-cation hybrid perovskites," *Chem. Mater.* **33**, 2769–2776 (2021).
- ²⁶Y. Zhou, H. Sternlicht, and N. P. Padture, "Transmission electron microscopy of halide perovskite materials and devices," *Joule* **3**, 641–661 (2019).
- ²⁷T. Nakamuro, M. Sakakibara, H. Nada, K. Harano, and E. Nakamura, "Capturing the moment of emergence of crystal nucleus from disorder," *J. Am. Chem. Soc.* **143**, 1763–1767 (2021).
- ²⁸M. K. Uppal, S. Ramasesha, and C. N. R. Rao, "Computer simulation of polytypes," *Acta Crystallogr. Sect. A* **36**, 356–361 (1980).
- ²⁹M. Moody, J. R. Ray, and A. Rahman, "Close-packed (polytypic) structures in molecular-dynamics simulations," *Phys. Rev. B* **35**, 557–570 (1987).
- ³⁰P. R. t. Wolde and D. Frenkel, "Enhancement of protein crystal nucleation by critical density fluctuations," *Science* **277**, 1975–1978 (1997).
- ³¹S. Piana, M. Reyhani, and J. D. Gale, "Simulating micrometre-scale crystal growth from solution," *Nature* **438**, 70–73 (2005).
- ³²J. Anwar and D. Zahn, "Uncovering molecular processes in crystal nucleation and growth by using molecular simulation," *Angew. Chem., Int. Ed.* **50**, 1996–2013 (2011).
- ³³D. Chakraborty and G. N. Patey, "How crystals nucleate and grow in aqueous NaCl solution," *J. Phys. Chem. Lett.* **4**, 573–578 (2013).
- ³⁴J. R. Espinosa, C. Vega, C. Valeriani, and E. Sanz, "Seeding approach to crystal nucleation," *J. Chem. Phys.* **144**, 034501 (2016).
- ³⁵L. Lupi, A. Hudait, B. Peters, M. Grünwald, R. Gotchy Mullen, A. H. Nguyen, and V. Molinero, "Role of stacking disorder in ice nucleation," *Nature* **551**, 218–222 (2017).
- ³⁶C. G. Bischak, M. Lai, Z. Fan, D. Lu, P. David, D. Dong, H. Chen, A. S. Etman, T. Lei, J. Sun, M. Grünwald, D. T. Limmer, P. Yang, and N. S. Ginsberg, "Liquid-like interfaces mediate structural phase transitions in lead halide perovskites," *Matter* **3**, 534–545 (2020).
- ³⁷W. Humphrey, A. Dalke, and K. Schulten, "VMD: Visual molecular dynamics," *J. Mol. Graphics* **14**, 33–38 (1996).
- ³⁸S. I. Seok, M. Grätzel, and N.-G. Park, "Methodologies toward highly efficient perovskite solar cells," *Small* **14**, 1704177 (2018).
- ³⁹P. Ren and J. W. Ponder, "Consistent treatment of inter- and intramolecular polarization in molecular mechanics calculations," *J. Comput. Chem.* **23**, 1497–1506 (2002).
- ⁴⁰J. C. Wu, J.-P. Piquemal, R. Chaudret, P. Reinhardt, and P. Ren, "Polarizable molecular dynamics simulation of Zn(II) in water using the AMOEBA force field," *J. Chem. Theory Comput.* **6**, 2059–2070 (2010).
- ⁴¹P. Ren, C. Wu, and J. W. Ponder, "Polarizable atomic multipole-based molecular mechanics for organic molecules," *J. Chem. Theory Comput.* **7**, 3143–3161 (2011).
- ⁴²J. A. Rackers, Z. Wang, C. Lu, M. L. Laury, L. Lagardère, M. J. Schnieders, J.-P. Piquemal, P. Ren, and J. W. Ponder, "Tinker 8: Software tools for molecular design," *J. Chem. Theory Comput.* **14**, 5273–5289 (2018).
- ⁴³Y. Shi, Z. Xia, J. Zhang, R. Best, C. Wu, J. W. Ponder, and P. Ren, "Polarizable atomic multipole-based AMOEBA force field for proteins," *J. Chem. Theory Comput.* **9**, 4046–4063 (2013).
- ⁴⁴Z. Wang, *Tinker9: Next Generation of Tinker with GPU Support* (Washington University, St. Louis, 2021).
- ⁴⁵P. V. G. M. Rathnayake, S. Bernardi, and A. Widmer-Cooper, "Evaluation of the AMOEBA force field for simulating metal halide perovskites in the solid state and in solution," *J. Chem. Phys.* **152**, 024117 (2020).
- ⁴⁶O. Adjou, L. Lagardère, L.-H. Jolly, A. Durocher, T. Very, I. Dupays, Z. Wang, T. J. Inizan, F. Célerse, P. Ren, J. W. Ponder, and J.-P. Piquemal, "Tinker-HP: Accelerating molecular dynamics simulations of large complex systems with advanced point dipole polarizable force fields using GPUs and multi-GPU systems," *J. Chem. Theory Comput.* **17**, 2034–2053 (2021).
- ⁴⁷P. Ahlawat, M. I. Dar, P. Piaggi, M. Grätzel, M. Parrinello, and U. Rothlisberger, "Atomistic mechanism of the nucleation of methylammonium lead iodide perovskite from solution," *Chem. Mater.* **32**, 529–536 (2020).

- ⁴⁸T. Bu, L. K. Ono, J. Li, J. Su, G. Tong, W. Zhang, Y. Liu, J. Zhang, J. Chang, S. Kazaoui, F. Huang, Y.-B. Cheng, and Y. Qi, "Modulating crystal growth of formamidinium-caesium perovskites for over 200 cm² photovoltaic sub-modules," *Nat. Energy* **7**, 528–536 (2022).
- ⁴⁹H. T. Pham, T. Duong, K. J. Weber, and J. Wong-Leung, "Insights into twinning formation in cubic and tetragonal multi-cation mixed-halide perovskite," *ACS Mater. Lett.* **2**, 415–424 (2020).
- ⁵⁰H. T. Pham, Y. Yin, G. Andersson, K. J. Weber, T. Duong, and J. Wong-Leung, "Unraveling the influence of CsCl/MACl on the formation of nanotwins, stacking faults and cubic supercell structure in FA-based perovskite solar cells," *Nano Energy* **87**, 106226 (2021).
- ⁵¹W. Li, M. U. Rothmann, Y. Zhu, W. Chen, C. Yang, Y. Yuan, Y. Y. Choo, X. Wen, Y.-B. Cheng, U. Bach, and J. Etheridge, "The critical role of composition-dependent intragrain planar defects in the performance of MA1-xFAxPbI3 perovskite solar cells," *Nat. Energy* **6**, 624–632 (2021).
- ⁵²J. Tian, D. B. Cordes, A. M. Z. Slawin, E. Zysman-Colman, and F. D. Morrison, "Progressive polytypism and bandgap tuning in azetidinium lead halide perovskites," *Inorg. Chem.* **60**, 12247–12254 (2021).
- ⁵³J. G. Kirkwood, "Statistical mechanics of fluid mixtures," *J. Chem. Phys.* **3**, 300–313 (1935).
- ⁵⁴D. Frenkel and B. Smit, *Understanding Molecular Simulation: From Algorithms to Applications*, 2nd ed., *Computational Science Series No. 1* (Academic Press, San Diego, CA, 2002).
- ⁵⁵M. Salvalaglio, T. Vetter, F. Giberti, M. Mazzotti, and M. Parrinello, "Uncovering molecular details of urea crystal growth in the presence of additives," *J. Am. Chem. Soc.* **134**, 17221–17233 (2012).
- ⁵⁶D. Meggiolaro, E. Mosconi, and F. De Angelis, "Formation of surface defects dominates ion migration in lead-halide perovskites," *ACS Energy Lett.* **4**, 779–785 (2019).
- ⁵⁷S. G. Motti, D. Meggiolaro, A. J. Barker, E. Mosconi, C. A. R. Perini, J. M. Ball, M. Gandini, M. Kim, F. De Angelis, and A. Petrozza, "Controlling competing photochemical reactions stabilizes perovskite solar cells," *Nat. Photonics* **13**, 532–539 (2019).
- ⁵⁸K. Momma and F. Izumi, "VESTA 3 for three-dimensional visualization of crystal, volumetric and morphology data," *J. Appl. Crystallogr.* **44**, 1272–1276 (2011).
- ⁵⁹J.-G. Cheng, J. A. Alonso, E. Suard, J.-S. Zhou, and J. B. Goodenough, "A new perovskite polytype in the high-pressure sequence of BaR₂O₃," *J. Am. Chem. Soc.* **131**, 7461–7469 (2009).
- ⁶⁰C.-Q. Jin, J.-S. Zhou, J. B. Goodenough, Q. Q. Liu, J. G. Zhao, L. X. Yang, Y. Yu, R. C. Yu, T. Katsura, A. Shatskiy, and E. Ito, "High-pressure synthesis of the cubic perovskite BaRuO₃ and evolution of ferromagnetism in ARuO₃ (A = Ca, Sr, Ba) ruthenates," *Proc. Natl. Acad. Sci. U. S. A.* **105**, 7115–7119 (2008).
- ⁶¹L. B. Pártay, C. Ortner, A. P. Bartók, C. J. Pickard, and G. Csányi, "Polytypism in the ground state structure of the Lennard-Jonesium," *Phys. Chem. Chem. Phys.* **19**, 19369–19376 (2017).
- ⁶²E. Marinari and G. Parisi, "Simulated tempering: A new Monte Carlo scheme," *Europhys. Lett.* **19**, 451–458 (1992).
- ⁶³U. H. Hansmann, "Parallel tempering algorithm for conformational studies of biological molecules," *Chem. Phys. Lett.* **281**, 140–150 (1997).
- ⁶⁴Y. Sugita and Y. Okamoto, "Replica-exchange molecular dynamics method for protein folding," *Chem. Phys. Lett.* **314**, 141–151 (1999).
- ⁶⁵Y. Sugita and Y. Okamoto, "Replica-exchange multicanonical algorithm and multicanonical replica-exchange method for simulating systems with rough energy landscape," *Chem. Phys. Lett.* **329**, 261–270 (2000).
- ⁶⁶G. Bussi, "Hamiltonian replica exchange in GROMACS: A flexible implementation," *Mol. Phys.* **112**, 379–384 (2014).
- ⁶⁷L. Pauling, "The principles determining the structure of complex ionic crystals," *J. Am. Chem. Soc.* **51**, 1010–1026 (1929).
- ⁶⁸M. R. Sorensen and A. F. Voter, "Temperature-accelerated dynamics for simulation of infrequent events," *J. Chem. Phys.* **112**, 9599–9606 (2000).
- ⁶⁹T.-Q. Yu and M. E. Tuckerman, "Temperature-accelerated method for exploring polymorphism in molecular crystals based on free energy," *Phys. Rev. Lett.* **107**, 015701 (2011).
- ⁷⁰J. Duncan, A. Harjunmaa, R. Terrell, R. Drautz, G. Henkelman, and J. Rogal, "Collective atomic displacements during complex phase boundary migration in solid-solid phase transformations," *Phys. Rev. Lett.* **116**, 035701 (2016).
- ⁷¹F. Montalenti and A. Voter, "Applying accelerated molecular dynamics to crystal growth," *Phys. Status Solidi B* **226**, 21–27 (2001).
- ⁷²J. B. Goodenough, J. A. Kafalas, and J. M. Longo, "High pressure synthesis," in *Preparative Methods in Solid State Chemistry* (Academic Press, 1972).
- ⁷³P. L. Gai and C. Rao, "Lattice imaging of close-packed structures by high resolution electron microscopy: ABO₃ perovskite polytypes," *Solid State Chemistry: Selected Papers of CNR Rao* (1995), pp. 56–65.
- ⁷⁴P. Hagenmuller, *Preparative Methods in Solid State Chemistry* (Elsevier Science, St. Louis, MO, 2014) oCLC: 1044715140.
- ⁷⁵L. T. Nguyen and R. J. Cava, "Hexagonal perovskites as quantum materials," *Chem. Rev.* **121**, 2935–2965 (2021).
- ⁷⁶Z.-A. Nan, L. Chen, Q. Liu, S.-H. Wang, Z.-X. Chen, S.-Y. Kang, J.-B. Ji, Y.-Y. Tan, Y. Hui, J.-W. Yan, Z.-X. Xie, W.-Z. Liang, B.-W. Mao, and Z.-Q. Tian, "Revealing phase evolution mechanism for stabilizing formamidinium-based lead halide perovskites by a key intermediate phase," *Chem* **7**, 2513–2526 (2021).
- ⁷⁷W. Kohn and L. J. Sham, "Self-consistent equations including exchange and correlation effects," *Phys. Rev.* **140**, A1133–A1138 (1965).
- ⁷⁸J. P. Perdew, K. Burke, and M. Ernzerhof, "Generalized gradient approximation made simple," *Phys. Rev. Lett.* **77**, 3865–3868 (1996).
- ⁷⁹J. VandeVondele, M. Krack, F. Mohamed, M. Parrinello, T. Chassaing, and J. Hutter, "Quickstep: Fast and accurate density functional calculations using a mixed Gaussian and plane waves approach," *Comput. Phys. Commun.* **167**, 103–128 (2005).
- ⁸⁰H. T. Pham, K. J. Weber, T. Duong, and J. Wong-Leung, "Impact of halide anions in CsX (X = I, Br, Cl) on the microstructure and photovoltaic performance of FAPbI₃-based perovskite solar cells," *Sol. RRL* **6**, 2200345 (2022).
- ⁸¹J.-W. Lee, D.-H. Kim, H.-S. Kim, S.-W. Seo, S. M. Cho, and N.-G. Park, "Formamidinium and cesium hybridization for photo- and moisture-stable perovskite solar cell," *Adv. Energy Mater.* **5**, 1501310 (2015).
- ⁸²M. Kim, G.-H. Kim, T. K. Lee, I. W. Choi, H. W. Choi, Y. Jo, Y. J. Yoon, J. W. Kim, J. Lee, D. Huh, H. Lee, S. K. Kwak, J. Y. Kim, and D. S. Kim, "Methylammonium chloride induces intermediate phase stabilization for efficient perovskite solar cells," *Joule* **3**, 2179–2192 (2019).
- ⁸³T. Baumeler, N. Arora, A. Hinderhofer, S. Akin, A. Greco, M. Abdi-Jalebi, R. Shivanna, R. Uchida, Y. Liu, F. Schreiber, S. M. Zakeeruddin, R. H. Friend, M. Graetzel, and M. I. Dar, "Minimizing the trade-off between photocurrent and photovoltage in triple-cation mixed-halide perovskite solar cells," *J. Phys. Chem. Lett.* **11**, 10188–10195 (2020).
- ⁸⁴G. Kim, H. Min, K. S. Lee, D. Y. Lee, S. M. Yoon, and S. I. Seok, "Impact of strain relaxation on performance of -formamidinium lead iodide perovskite solar cells," *Science* **370**, 108–112 (2020).
- ⁸⁵E. A. Duijnste, B. M. Gallant, P. Holzhey, D. J. Kubicki, S. Collavini, B. K. Sturtdza, H. C. Sansom, J. Smith, M. J. Gutmann, S. Saha, M. Gedda, M. I. Nugraha, M. Kober-Czerny, C. Xia, A. D. Wright, Y.-H. Lin, A. J. Ramadan, A. Matzen, E. Y.-H. Hung, S. Seo, S. Zhou, J. Lim, T. D. Anthopoulos, M. R. Filip, M. B. Johnston, R. J. Nicholas, J. L. Delgado, and H. J. Snaith, "Understanding the degradation of methylammonium and its role in phase-stabilizing formamidinium lead triiodide," *J. Am. Chem. Soc.* **145**, 10275–10284 (2023).
- ⁸⁶S. Pronk and D. Frenkel, "Can stacking faults in hard-sphere crystals anneal out spontaneously?," *J. Chem. Phys.* **110**, 4589–4592 (1999).
- ⁸⁷L. Del Rosso, M. Celli, F. Grazzi, M. Catti, T. C. Hansen, A. D. Fortes, and L. Ulivi, "Cubic ice Ic without stacking defects obtained from ice XVII," *Nat. Mater.* **19**, 663–668 (2020).
- ⁸⁸X. Huang, L. Wang, K. Liu, L. Liao, H. Sun, J. Wang, X. Tian, Z. Xu, W. Wang, L. Liu, Y. Jiang, J. Chen, E. Wang, and X. Bai, "Tracking cubic ice at molecular resolution," *Nature* **617**, 86–91 (2023).
- ⁸⁹G. Ferraris, E. Makovicky, and S. Merlino, *Crystallography of Modular Materials* (Oxford University Press, 2008).
- ⁹⁰M. S. Shur, "Chapter 4 SiC transistors," in *Semiconductors and Semimetals* (Elsevier, 1998), Vol. 52, pp. 161–193.

- ⁹¹J. R. Weber, W. F. Koehl, J. B. Varley, A. Janotti, B. B. Buckley, C. G. Van De Walle, and D. D. Awschalom, "Defects in SiC for quantum computing," *J. Appl. Phys.* **109**, 102417 (2011).
- ⁹²T. Kong, K. Górnicka, S. Gołab, B. Wiendlocha, T. Klimczuk, and R. J. Cava, "A family of Pb-based superconductors with variable cubic to hexagonal packing," *J. Phys. Soc. Jpn.* **87**, 074711 (2018).
- ⁹³J. P. Zhang, D. J. Li, H. Shihahara, and L. D. Marks, "Structure and polytypes in thallium superconductors," *Supercond. Sci. Technol.* **1**, 132–136 (1988).
- ⁹⁴H. Luo, W. Xie, J. Tao, H. Inoue, A. Gyenis, J. W. Krizan, A. Yazdani, Y. Zhu, and R. J. Cava, "Polytypism, polymorphism, and superconductivity in TaSe_{2x}Te_x," *Proc. Natl. Acad. Sci. U. S. A.* **112**, E1174 (2015).
- ⁹⁵V. Heine, C. Cheng, and R. J. Needs, "The preference of silicon carbide for growth in the metastable cubic form," *J. Am. Ceram. Soc.* **74**, 2630–2633 (1991).
- ⁹⁶S. A. Lee, J. M. Ok, J. Lee, J. Hwang, S. Yoon, S. Park, S. Song, J. Bae, S. Park, H. N. Lee, and W. S. Choi, "Epitaxial stabilization of metastable 3C BaRuO₃ thin film with ferromagnetic non-fermi liquid phase," *Adv. Electron. Mater.* **7**, 2001111 (2021).